Analysis of the mixed state in $ErRh_4B_4$

J. P. Whitehead, H. Matsumoto, R. Teshima, and H. Umezawa
Theoretical Physics Institute, Department of Physics, The University of Alberta, Edmonton, Alberta, Canada T6G 2J1
(Received 22 November 1983)

An analysis of the mixed state in $ErRh_4B_4$ is presented and the results are compared with the recent measurements of the magnetic properties of single-crystal $ErRh_4B_4$. The analysis includes the shielding of the Er magnetic moment by the persistent current, the polarization of the conduction electrons by the Er magnetic moment, and the scattering of the conduction electrons by the spin fluctuations. Good agreement with both the hard- and easy-magnetization-axis measurements is obtained using a single value of κ_B in both directions. Unlike previous analysis, the formalism employed permits the analysis of the region in which the transition from the mixed state to the normal state is first order. The jump in the magnetization at H_{c2} is computed as a function of temperature.

I. INTRODUCTION

Recent experiments on a single crystal of $ErRh_4B_4$ have revealed many peculiar properties. The upper critical field measured with respect to the easy-magnetization axis is seen to have a peak value of about 2 kG at around $T\simeq 5.5$ K,[1] while the upper critical field relative to the hard-magnetization axis is similar to that observed for nonmagnetic superconductors with a peak value of about 10 kG.[2] Also, the magnetization curves measured with respect to the easy axis show that the transition from the mixed state to the normal state becomes first order at around $T\simeq 3.5$ K.[2] In this paper we present an analysis of the mixed state based on the formalism presented in Ref. 3, modified to take account of the *d-f* interaction in the manner outlined in Ref. 4. The formalism presented in Ref. 4 demonstrated how the polarization of the conduction electrons and the scattering by the localized-spin fluctuations arising from the *d-f* interaction (sometimes referred to as the *s-f* interaction) could be calculated in a consistent manner and the resultant free energy evaluated. In this analysis we assume that the superconducting properties of the system may be assumed isotropic and that the observed anisotropy arises purely from the anisotropy of the interaction between the rare-earth (RE) magnetic ions.

The arrangement of the paper is as follows. In Sec. II we summarize the formulas derived in Ref. 4 to take account of the modification to the superconducting electrons arising from the *d-f* interaction in the presence of an applied field. In Sec. III we outline how the results of Ref. 3 may be extended to incorporate the *d-f* interaction; in particular, how the free energy, the equilibrium flux density, the magnetization, and the upper and lower critical fields are calculated. An important point in this work is that the formalism presented in this section is able, without modification, to treat the temperature domain wherein the transition from the mixed state to the normal state is first order. This allows us to analyze the magnetic properties of the mixed state over the whole range of temperatures. Section IV contains a discussion of the various parameters required for the analysis and to what extent they can be determined by existing measurements. In Sec. V we present the upper and lower critical fields calculated both with and without the effect of the scattering of the conduction electrons by fluctuations in the localized spins. The analysis includes the domain in which the transition at H_{c2} is first order. In Sec. VI several magnetization curves, calculated both with and without the effect of the scattering of the conduction electrons by the fluctuations of the localized spins, are presented and discussed. The nature of the first-order transition is clearly seen and the calculated jump in the magnetization is plotted as a function of temperature. Section VII contains some conclusions. The results presented in Secs. V and VI are seen to be in good agreement with experiment.

II. SUPERCONDUCTING PROPERTIES AND THE INTERNAL FIELDS

The rare-earth ternary superconductors such as $ErRh_4B_4$ may be described by the following Hamiltonian density:

$$\mathscr{H}(x)=\mathscr{H}_{\rm BCS}(x)-\tfrac{1}{2}\vec{\mathrm{M}}\cdot\gamma_0(-i\vec{\nabla})\vec{\mathrm{M}}-I\vec{\mathrm{M}}\psi^\dagger\vec{\sigma}\psi$$
$$-\vec{\mathrm{M}}\cdot\vec{\mathrm{B}}+\mu_B\psi^\dagger\vec{\sigma}\psi\cdot\vec{\mathrm{B}}+\frac{1}{8\pi}(|\vec{\mathrm{B}}|^2+|\vec{\mathrm{E}}|^2)\,. \quad (2.1)$$

The field ψ denotes the electron field, $\vec{\mathrm{B}}$ denotes the magnetic induction ($\vec{\mathrm{B}}=\vec{\nabla}\times\vec{\mathrm{A}}$), $\vec{\mathrm{E}}$ denotes the electric field, while $\vec{\mathrm{M}}$ denotes the magnetic moment density of the localized spins:

$$\vec{\mathrm{M}}(\vec{\mathrm{x}})=\sum_n g_J J\mu_B\vec{\mathrm{S}}\delta(\vec{\mathrm{x}}-\vec{\mathrm{R}}_n)\,, \quad (2.2)$$

where $\{\vec{\mathrm{R}}_n\}$ denotes the lattice points of the magnetic ions and $\mathscr{H}_{\rm BCS}$ is the BCS Hamiltonian with the minimal electromagnetic interaction:

$$\mathscr{H}_{\rm BCS}(x)=\psi^\dagger\epsilon(-i[\vec{\nabla}-(ie/\hbar c)\vec{\mathrm{A}}])\psi$$
$$-V\psi_\uparrow^\dagger\psi_\downarrow^\dagger\psi_\downarrow\psi_\uparrow+\delta\epsilon\,\psi^\dagger\psi\,. \quad (2.3)$$

The electron spectrum denoted by $\epsilon(\vec{\mathrm{k}})$ will be assumed to be parabolic and therefore we have

$$\epsilon(-i[\vec{\nabla}-(ie/\hbar c)\vec{A}])=-\frac{1}{2m}([\vec{\nabla}-(ie/\hbar c)\vec{A}]^2+k_F^2)\ . \tag{2.4}$$

The superconducting properties arising from this Hamiltonian have been discussed in the preceding paper[4] by three of the present authors and may be summarized by the following expressions for the gap, the field-dependent condensation energy, and the London penetration depth:

$$\frac{\Delta(T;H)}{\Delta_0}=s(t;H)\mathscr{D}(t/s(t;H);\mu/s(t;H))\ , \tag{2.5}$$

$$\frac{H_c(T;H)}{H_{c0}}=s(t;H)\mathscr{H}(t/s(t;H);\mu/s(t;H))\ , \tag{2.6}$$

and

$$\frac{\lambda_L(T;H)}{\lambda_{L0}}=\mathscr{L}(t/s(t;H);\mu/s(t;H))\ . \tag{2.7}$$

Here t denotes the reduced temperature $t=T/T_c$, H denotes a certain internal field, which will be specified later, and the functions $\mathscr{D}$, $\mathscr{H}$, and $\mathscr{L}$ are defined by the expressions

$$\ln\mathscr{D}(t;\mu)=-\Phi_1\left[\frac{\pi e^{-\gamma}}{t}\mathscr{D}(t;\mu);\frac{\pi e^{-\gamma}}{t}\mu\right]\ , \tag{2.8}$$

$$\mathscr{L}^{-2}(t;\mu)=1-\Phi_2\left[\frac{\pi e^{-\gamma}}{t}\mathscr{D}(t;\mu);\frac{\pi e^{-\gamma}}{t}\mu\right]\ , \tag{2.9}$$

and

$$\mathscr{H}^2(t;\mu)=\mathscr{D}(t;\mu)-\frac{2\pi^2}{3}\left[\frac{t^2}{\pi e^{-\gamma}}-\frac{3}{\pi^2}\mathscr{D}^2(t;\mu)\Phi_3\left[\frac{\pi e^{-\gamma}}{t}\mathscr{D}(t;\mu);\frac{\pi e^{-\gamma}}{t}\mu\right]-\frac{3\mu}{\pi^2}\mathscr{D}(t;\mu)\Phi_4\left[\frac{\pi e^{-\gamma}}{t}\mathscr{D}(t;\mu);\frac{\pi e^{-\gamma}}{t}\mu\right]\right]\ , \tag{2.10}$$

where the functions $\{\Phi_i\}$ may be expressed in terms of the real part of certain complex integrals:

$$\Phi_i(x;y)=\frac{x}{4}\mathrm{Re}\int_{-\infty}^{+\infty}dz\,T_i(z)\cosh^{-2}[\tfrac{1}{2}(xz+y)] \tag{2.11}$$

evaluated along the contour shown in Fig. 1 with

$$T_1(z)=\ln[z+(z^2-1)^{1/2}]\ , \tag{2.12}$$

$$T_2(z)=\frac{z}{(z^2-1)^{1/2}}\ , \tag{2.13}$$

$$T_3(z)=z(z^2-1)^{1/2}\ , \tag{2.14}$$

$$T_4(z)=(z^2-1)^{1/2}\ . \tag{2.15}$$

The scale factor $s(t;H)$ arises from the scattering of the electrons by the localized-spin fluctuations and may be expressed in terms of the temperature- and field-dependent effective coupling constant as

$$s(t;H)=\exp\left[\frac{1}{g(t;H)N(0)}-\frac{1}{g_0N(0)}\right]\ , \tag{2.16}$$

where $g(t;H)$ was shown to be of the form

$$g(t;H)=\int\frac{d\Omega_k}{4\pi}\times\int\frac{d\Omega_p}{4\pi}\left[V-I^2\sum_i\chi_{ii}(\vec{p}-\vec{k})\right]_{|\vec{p}|=|\vec{k}|=k_F} \tag{2.17}$$

and g_0 is defined as

$$g_0\equiv g(t=1;H=0)\ . \tag{2.18}$$

Here χ denotes the static susceptibility of the localized-spin system calculated in the superconducting state.

The parameter μ arises from the spin splitting of conduction electrons and is expressed by

$$\mu=I\langle M_3\rangle/\Delta_0\ . \tag{2.19}$$

The expression for the electron current is given by[5]

$$\vec{j}(x)=\frac{1}{\lambda_L^2(t;H)}C(-i\vec{\nabla})[\vec{A}(x)-(\hbar c/e)\vec{\nabla}f(x)]\ , \tag{2.20}$$

where $\vec{A}$ denotes the vector potential, $f(x)$ is one-half the phase of the superconducting electrons, and $C(-i\vec{\nabla})$ is the nonlocal kernel. Here $C(-i\vec{\nabla})$ is given by[5]

$$C(-i\vec{\nabla})=\exp\left[-\frac{\xi^2(t)|\vec{k}|^2}{2}\right]\ , \tag{2.21}$$

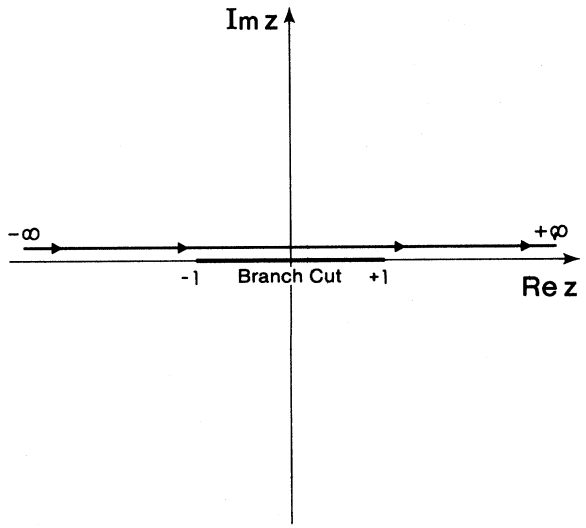

FIG. 1. Contour for the complex integrals contained in the expressions for $\{\Phi_i(x;y)\}$, $i=1,4$.

where $\xi(t;H)$ is the coherence length and is assumed to be given by[4,5]

$$\xi(t;H)=\frac{\hbar v_F}{\pi\Delta(t;H)} . \tag{2.22}$$

The internal fields $\vec{B}$, $\vec{H}(=\vec{B}-4\pi\vec{M})$, and $\vec{M}$ may be obtained by means of mean-field theory:

$$\langle M_3\rangle = g_J\mu_B JNB_J(g_J J\mu_B\beta\,|\,H_M\,|\,) , \tag{2.23}$$

where B_J is the Brillouin function and H_M is the mean field given by

$$H_M=\langle B_3\rangle+(\gamma_0+I^2\chi_\sigma)\langle M_3\rangle , \tag{2.24a}$$

which together with the Maxwell equation

$$\vec{\nabla}\times\vec{H}(x)=-\frac{1}{\lambda_L^2}C(-i\vec{\nabla})[\vec{A}(x)-(\hbar c/e)\vec{\nabla}f] , \tag{2.24b}$$

that is

$$-\nabla^2\vec{H}(x)=-\frac{1}{\lambda_L^2}C(-i\vec{\nabla})[\vec{B}(x)-(\hbar c/e)\vec{\nabla}\times\vec{\nabla}f] \tag{2.25}$$

allows the calculation of the magnetization $\langle M_3\rangle$ for a given vortex density $\vec{n}(x)$ with $\vec{n}(x)$ defined as

$$\vec{n}(x)=\frac{1}{\pi}\vec{\nabla}\times\vec{\nabla}f(x) . \tag{2.26}$$

The inverse susceptibilities (χ_{ij}^{-1}) may be calculated from a linear-response agreement within the context of mean-field theory as[4]

$$\chi^{-1}=\begin{bmatrix} H_M/\langle M_3\rangle & 0 & 0 \\ 0 & H_M/\langle M_3\rangle & 0 \\ 0 & 0 & T/C\alpha_J \end{bmatrix}-\tilde{\gamma}(-i\vec{\nabla}) , \tag{2.27}$$

where C denotes the Curie constant,

$$C=g_J^2\mu_B^2NJ(J+1)/3k_B , \tag{2.28}$$

while α_J is given by

$$\alpha_J=\frac{3J}{J+1}B_J'(\beta g_J\mu_B J\,|\,H_M\,|\,) , \tag{2.29}$$

and $\tilde{\gamma}(\vec{k})$ is given by

$$\tilde{\gamma}(\vec{k})=\gamma_0(\vec{k})+I^2\chi_\sigma+4\pi-4\pi\frac{\lambda_L^{-2}C(\vec{k})}{|\vec{k}|^2+\lambda_L^{-2}C(\vec{k})} . \tag{2.30}$$

The last term in Eq. (2.30) represents the shielding of the magnetic spins by the persistent current.[6]

In order to compute the superconducting quantities Δ, H_c, and λ_L, we make the following approximations. First, we replace the fields $B(x)$, $M(x)$, etc. by their spatial averages. Then the spin-splitting parameter μ may be calculated as a function of the average vortex density n given by

$$n=\frac{1}{V}\int_V d^3x\ \vec{\nabla}\times\vec{\nabla}f(x)\cdot\vec{e}_3 \tag{2.31}$$

from the equation for the mean magnetic moment per unit volume obtained from Eq. (2.23) with H_M given by

$$H_M=n\phi+(\gamma_0+I^2\chi_\sigma)\langle M_3\rangle . \tag{2.32}$$

Second, we assume that spin susceptibility χ_σ has the same value in both the normal and superconducting state and hence that γ_0 may be parametrized as

$$(\gamma_0+I^2\chi_\sigma-4\pi)_{ij}=\left[\frac{T_m^{(i)}}{C}-\frac{D}{C}|\vec{k}|^2[1+\tfrac{3}{2}\alpha(1-\cos^2\theta)]\right]\delta_{ij} , \tag{2.33}$$

where $T_m^{(i)}=T_m^{(a)}(T_m^{(c)})$ if i lies along the easy-a (hard-c) axis and the parameter α provides for a degree of anisotropy in momentum space. The angle θ denotes the angle between $\vec{k}$ and the direction of the spin modulation, which may appear in sinusoidal phase. From Eq. (2.33) together with Eqs. (2.27) and (2.30), we can compute $g(T;H)$ from Eq. (2.17) to give[4]

$$g(t;n)=1-\frac{I^2}{g_0}[G^{(a)}(\epsilon_\perp^{(a)}(t;n))+G^{(a)}(\epsilon_{||}^{(a)}(t;n))-2G^{(a)}(\epsilon^{(a)}(t=1))]-\frac{I^2}{g_0}[G^{(c)}(\epsilon_\perp^{(c)}(t;n))-G^{(c)}(\epsilon^{(c)}(t=1))] \tag{2.34a}$$

when the field is applied along the easy axis, and

$$g(t;n)=1-\frac{I^2}{g_0}[2G^{(a)}(\epsilon_\perp^{(a)}(t;n))-2G^{(a)}(\epsilon^{(a)}(t=1))]-\frac{I^2}{g_0}[G^{(c)}(\epsilon_{||}^{(c)}(t;n))-2G^{(c)}(\epsilon^{(c)}(t=1))] \tag{2.34b}$$

when the field is along the hard axis. Here

$$G^{(i)}(\epsilon)=\frac{c^{(i)}}{8\pi d_f^{(i)}(1+\alpha)}\left[\ln\left|\frac{d_f^{(i)2}(1+\alpha)+d_f^{(i)}[\epsilon+d^{(i)}(1+\alpha)]+d^{(i)}(\epsilon+c^{(i)})}{d^{(i)}(\epsilon+c^{(i)})}\right|\right.$$
$$+\frac{d^{(i)}(1+\alpha)-\epsilon}{[D_i(\epsilon)]^{1/2}}\left[\ln\left|\frac{2d_f^{(i)}(1+\alpha)+\epsilon+d_f^{(i)}(1+\alpha)-[D_i(\epsilon)]^{1/2}}{2d_f^{(i)}(1+\alpha)+\epsilon+d_f^{(i)}(1+\alpha)+[D_i(\epsilon)]^{1/2}}\right|\right.$$
$$\left.\left.-\ln\left|\frac{\epsilon+d_f^{(i)}(1+\alpha)-[D_i(\epsilon)]^{1/2}}{\epsilon+d_f^{(i)}(1+\alpha)+[D_i(\epsilon)]^{1/2}}\right|\right]\right] \quad \text{for } D_i>0 , \tag{2.35a}$$

and

$$G^{(i)}(\epsilon)=\frac{c^{(i)}}{8\pi d_f^{(i)}(1+\alpha)}\left\{\ln\left|\frac{d_f^{(i)2}(1+\alpha)+d_f^{(i)}[\epsilon+d^{(i)}(1+\alpha)]+d^{(i)}(\epsilon+c^{(i)})}{d^{(i)}(\epsilon+c^{(i)})}\right|\right.$$
$$+2\frac{d_i(1+\alpha)-\epsilon}{[-D_i(\epsilon)]^{1/2}}\left[\tan^{-1}\left[\frac{2d_f^{(i)}(1+\alpha)+\epsilon+d_f^{(i)}(1+\alpha)}{[-D_i(\epsilon)]^{1/2}}\right]\right.$$
$$\left.\left.-\tan^{-1}\left[\frac{\epsilon+d_f^{(i)}(1+\alpha)}{[-D_i(\epsilon)]^{1/2}}\right]\right]\right\}\quad\text{for } D_i<0\ . \tag{2.35b}$$

The dimensionless quantities used in the above expression are given by

$$c^{(i)}=\frac{4\pi C}{T_m^{(i)}},\quad i=(a\text{ or }c)$$
$$d_f^{(i)}=4\frac{Dk_f^2}{T_m^{(i)}},\quad d^{(i)}=\frac{D\lambda_L^{-2}}{T_m^{(i)}}\ , \tag{2.35c}$$
$$D_i(\epsilon)=[\epsilon+d^{(i)}(1+\alpha)]^2-4d_i(1+\alpha)c_i\ ,$$

and $\epsilon_\perp$ and $\epsilon_{||}$ are given by

$$\epsilon_\perp^{(i)}(t;n)=c^{(i)}\left[\frac{n}{4\pi\langle M_3\rangle}-1\right]+\left[\frac{t_m}{t_m^{(i)}}-1\right] \tag{2.35d}$$

and

$$\epsilon_{||}^{(i)}(t;n)=\left[\frac{t}{\alpha_J t_m^{(i)}}-1\right], \tag{2.35e}$$

where $t_m=t_m^{(a)}$ ($t_m^{(c)}$) when the field is applied along the easy (hard axis) and $\epsilon^{(i)}(t)$ is given by

$$\epsilon^{(i)}(t)\equiv\epsilon_\perp^{(i)}(t;n=0)=\epsilon_{||}^{(i)}(t;n=0)\ . \tag{2.35f}$$

In deriving this expression for $g(t;n)$, we have made use of the London limit [$C(k)=1$] and replaced the anisotropy in the momentum dependence, $\frac{3}{2}\alpha(1+\cos^2\theta)$, by its spherical average α as discussed in Ref. 4.

Thus μ and s may be calculated for a given n at a particular temperature and the quantities Δ, H_c, and λ_L may be computed by means of Eqs. (2.5), (2.6), and (2.7), respectively. Graphs showing the dependence of these quantities on the internal field $H=n\phi-4\pi\langle M\rangle$ were presented in Ref. 4.

III. FREE ENERGY IN THE MIXED STATE

The expression for the free energy, obtained from the Hamiltonian given by Eq. (2.1), was derived in Ref. 4. The result may be written as

$$F_s(n)=\frac{1}{V}\int d^3x\left[\frac{1}{8\pi}\vec{n}(x)\phi\cdot\langle\vec{H}(x)\rangle+\tfrac{1}{2}\vec{H}_M(x)\cdot\langle\vec{M}(x)\rangle\right.$$
$$-\frac{N}{\beta}\ln Z_J[g_J\mu_B J\beta\,|\,\vec{H}_M(x)\,|\,]$$
$$\left.-\frac{H_c^2}{8\pi}+E_{\text{core}}(x)\right], \tag{3.1}$$
$$Z_J(x)=\sinh\left[\frac{2J+1}{2J}x\right]\Big/\sinh\left[\frac{1}{2J}x\right].$$

As was noted in Ref. 4, this has an identical structure to that presented in Ref. 3, although the individual terms are more complicated due to the effects of the d-f interaction. The similarity in the structure between this expression and that presented in Ref. 3 means that many of the earlier results may be used with little modification. In particular, if we assume a triangular array of vortices such that

$$\vec{n}(x)=\sum_i\vec{e}_3\delta^2(\vec{x}-\vec{\xi}_i)\ , \tag{3.2}$$

where $\{\vec{\xi}_i\}$ denotes the position of the vortices, then, following Ref. 3, the first term appearing in Eq. (3.1) may be calculated to be

$$\frac{1}{V}\int d^3x\frac{1}{8\pi}\vec{n}(x)\cdot\langle\vec{H}(x)\rangle=\frac{n\phi}{8\pi}[n\phi-4\pi\langle M_3\rangle+h(0)]\ , \tag{3.3}$$

where $h(0)$ is given by

$$h(0)=n\phi\sum_{\vec{K}\ (\neq\vec{0})}\frac{\lambda_L^{-2}(t;n)C(\vec{K})}{[\,|\vec{K}|^2+[1+4\pi\chi(\vec{K})]\lambda_L^{-2}(t;n)C(\vec{K})}\ , \tag{3.4}$$

and the set $\{\vec{K}\}$ denotes the reciprocal-lattice vectors of the vortex lattice.

Similarly, the core energy, which represents the energy arising from the nonlinear effect of the vector potential and the phase $f(x)$, may be approximated by

$$\frac{1}{V}\int d^3x\,E_{\text{core}}(x)=n[E_1-E_2b^{\text{int}}(n)]\ , \tag{3.5}$$

where $b^{\text{int}}(n)$ is given by

$$b^{\text{int}}(n)=n\phi\left[1+\sum_{\vec{K}\,(\neq\vec{0})}\frac{[1+4\pi\chi(\vec{K})]\lambda_L^{-2}(t;n)C(\vec{K})}{[\,|\vec{K}|^2+[1+4\pi\chi(\vec{K})]\lambda_L^{-2}(t;n)C(\vec{K})}\right]-\phi\int\frac{d^2k}{(2\pi)^2}\frac{[1+4\pi\chi(\vec{k})]\lambda_L^{-2}(t;n)C(\vec{k})}{|\vec{k}|^2+[1+4\pi\chi(\vec{k})]\lambda_L^{-2}(t;n)C(\vec{k})}\,, \tag{3.6}$$

and E_1 is estimated using the virial theorem[3,7] and is given by

$$E_1=\frac{\hbar c^2}{32e^2}\frac{1}{\lambda_L^2(t;n)}\,. \tag{3.7}$$

Equation (3.5) may then be written as

$$E_{\text{core}}=\frac{\phi^2}{8\pi\lambda_L^2(t;n)}\left[\frac{1}{4\pi}-\epsilon_2 b_{\text{int}}(n)\right]. \tag{3.8}$$

The parameter ϵ_2, characterizing multiple vortex effects, is chosen by the requirement that there exists a second-order transition point to the normal state.

The remaining terms, the condensation energy of the superconducting electrons and the free energy of the magnetic ions, may be obtained from the expressions given in the preceding section. Thus we arrive at the following expression for the free energy $F_s(n)$ for a given vortex density n:

$$F_s(n)=\frac{n\phi}{8\pi}\left[n\phi+h(0)+\frac{\phi}{\lambda_L^2(n;t)}\left[\frac{1}{4\pi}-\epsilon_2 b_{\text{int}}(n)\right]\right]+F_m(\tilde{\gamma};n)-\frac{H_c^2(t;n)}{8\pi}\,, \tag{3.9}$$

where

$$F_m(\tilde{\gamma};n)=\tfrac{1}{2}\tilde{\gamma}(\vec{k}=0)\langle M_3\rangle^2-\frac{N}{\beta}\ln Z_J\{g_J\mu_B J\beta[n\phi+\tilde{\gamma}(0)\langle M_3\rangle]\}\,. \tag{3.10}$$

Before discussing the determination of the magnetic properties, it is worthwhile to consider how the various quantities appearing in the expression for the free energy given by Eq. (3.9) are affected by *d-f* interaction. First, the London penetration depth and the condensation energy, appearing in the third and fifth terms of Eq. (3.9), respectively, now depend on the polarization of the RE magnetic ions induced by the magnetic fields generated by the vortex lattice. Second, the superconducting currents generated by vortices will be modified by the change in the coherence length given by Eq. (2.22). Such effects were not included in the analysis of the mixed state presented in Ref. 3, where it was argued that the effect of the *d-f* interaction was small and could be incorporated as a *temperature-independent* renormalization of the various parameters.

With the free energy calculated as a function of the vortex density, the applied field H may be obtained as a function of the vortex density from the Gibbs free energy $G_s(n)$,

$$G_s(n)=F_s(n)-\frac{n\phi}{4\pi}H\,, \tag{3.11}$$

by the thermodynamic requirement that $G_s(n)$ be minimized with respect to the vortex density n. Thus we have

$$\left.\frac{\partial G_s(n)}{\partial n}\right|_t=0\,, \tag{3.12a}$$

which leads to

$$H(n)=\frac{4\pi}{\phi}\left.\frac{\partial F_s(n)}{\partial n}\right|_t. \tag{3.12b}$$

The second-order transition to the normal state occurs when $n=n_c^0$, such that

$$G_s(n_c^0)=G_N(H_{c2}^0)\,, \tag{3.13}$$

$$n_c^0\phi=H_{c2}^0+4\pi M_{H_{c2}^0}\,, \tag{3.14}$$

where H_{c2}^0 is defined by

$$H_{c2}^0=H(n_c^0)\,, \tag{3.15}$$

while $G_N(H)$ is the free energy of the normal state given by[4]

$$G_N=-\frac{H^2}{8\pi}+F_m(\gamma;H) \tag{3.16}$$

with

$$F_m(\gamma;H)=\tfrac{1}{2}(\gamma_0+I\chi_\sigma+4\pi)M_H^2-\frac{N}{\beta}\ln Z_J\{g_J\mu_B J\beta[H+(\gamma_0+I\chi_\sigma+4\pi)M_H]\}\,, \tag{3.17}$$

and M_H is obtained from

$$M_H=g_J\mu_B JNB_J\{g_J\mu_B J\beta[H+(\gamma_0+I\chi_\sigma+4\pi)M_H]\}\,. \tag{3.18}$$

Equations (3.13) and (3.14) serve to determine both the critical flux density n_c^0 together with the parameter ϵ_2.

If it is the case, as one normally finds in nonmagnetic type-II superconductors, that

$$G_s(n)<G_N(H(n)) \tag{3.19}$$

for

$$n<n_c^0\,, \tag{3.20}$$

then the transition from the mixed state to the normal state will be second order and H_{c2}^0 given by Eq. (3.14) will

correspond to the physically observed upper critical field which we denote by H_{c2}.

It can happen, as we will see later in specific instances, that

$$G_s(n)=G_N(H(n)) \tag{3.21}$$

for certain n satisfying

$$n<n_c^0 . \tag{3.22}$$

In this situation the observed critical flux density n_c is determined from Eq. (3.21) rather than (3.13) and (3.14). Then we have

$$n_c<n_c^0 , \tag{3.23}$$

while the observed upper critical field H_{c2} is given by

$$H_{c2}=H(n_c)>H_{c2}^0 \tag{3.24}$$

and the transition is first order, being accompanied by a jump in the magnetization similar to that shown in Fig. 2. We will discuss these rather peculiar effects in greater detail in later sections when we report on the results of various numerical calculations. It should be emphasized that the above change of the order of transition does not require any modification of the present formalism. What is assumed is that there is a point at which the second-order transition occurs. This determines the parameter ϵ_2, thus the theory naturally predicts the first-order transition if it occurs.

The value of the applied field from which transition from the pure Meissner state to the mixed state occurs may also be determined from Eq. (3.12b) as

$$H_{c1}^0=H(n=0) . \tag{3.25}$$

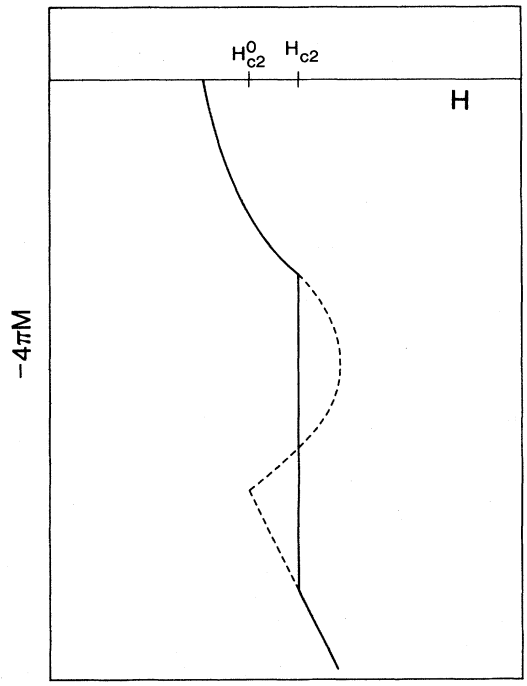

FIG. 2. Schematic illustration of the magnetization curve in the neighborhood of H_{c2} for a type-$II_{i,1}$ superconductor.

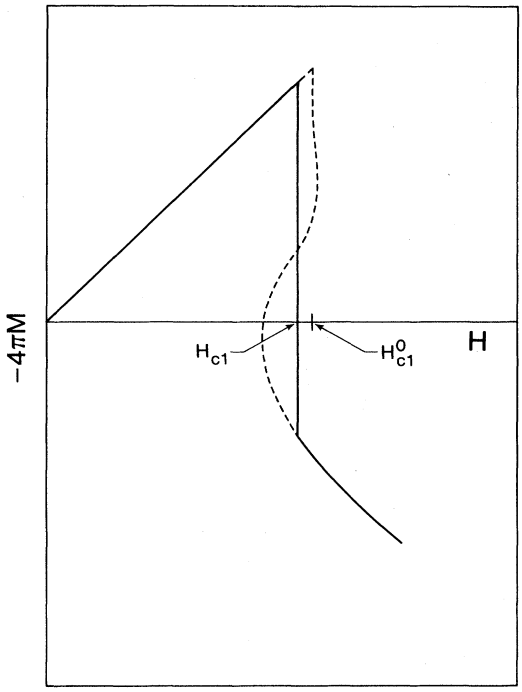

FIG. 3. Schematic illustration of the magnetization curve in the neighborhood of H_{c1} for a type-$II_{1,i}$ superconductor.

It may occur that the free energy in the mixed state may actually increase as the vortex density increases. In such a situation the magnetization curve will be similar to that shown in Fig. 3 and the transition will be of first order, and we will have that the observed lower critical field H_{c1} will be such that

$$H_{c1}<H_{c1}^0 . \tag{3.26}$$

Calculations in both nonmagnetic and magnetic superconductors indicate that the difference between H_{c1} and H_{c1}^0 is small and may be neglected for all practical purposes.

IV. PARAMETERS FOR $ErRh_4B_4$

In order to apply the formalism summarized in the preceding sections to the analysis of $ErRh_4B_4$, we need to know the various parameters that characterize the magnetic system, the superconducting system, and the degree of coupling between the two systems. The Curie constant C and the saturation magnetization may be obtained from the observed lattice constant, together with the values of J and g_J which may be assumed to have the same value as the free Er ion. The values given in Table I are in reason-

TABLE I. Experimental values for $ErRh_4B_4$.

$T_{c1}=8.7$ K	$J=\frac{15}{2}$
$T_{c2}=0.7$ K	$g_J=\frac{6}{5}$
$T_m^{(a)}=1.0$ K	$C=0.184$ K
$T_m^{(c)}=-20.0$ K	$4\pi g_J\mu_B JN=10.11$ kOe
$T_p=0.8$ K	$\frac{1}{T_c}\frac{dT_c(x)}{dx}=10.11$
$H_{c0}=1.4$ kG	

able agreement with those estimated from the inverse susceptibility measurements.[8] The Curie temperatures for the hard axis, $T_m^{(c)}$, and the easy axis, $T_m^{(a)}$, may be obtained from an extrapolation of the inverse susceptibility measurements measured with respect to the hard and easy axes, respectively.[8] The condensation energy $H_{c0}^2/8\pi$ may be estimated from the value obtained for $LuRh_4B_4$ [$H_{c0}(LuRh_4B_4)=1.85$ kOe] from specific-heat measurements[9] using the relation

$$\frac{T_c(\mathrm{Lu})}{T_c(\mathrm{Er})}=\frac{H_{c0}(\mathrm{Lu})}{H_{c0}(\mathrm{Er})} . \tag{4.1}$$

This yields a value for Er of around 1.4 kG. The parameter κ_B has been estimated experimentally to be around 4.[10] The value of the field normalization ϕ/λ_{L0}^2 may then be obtained from the relation

$$H_{c0}^2=\frac{3}{2}\frac{\kappa_B^2}{\pi^4}\left[\frac{\phi}{\lambda_{L0}^2}\right]^2 .$$

With the above values we have estimated $\lambda_{L0}\simeq 825$ Å. The value of $g_0N(0)$ is chosen to be around 0.3. The ratio I^2/g_0 may be estimated from the increase in the transition temperature as nonmagnetic impurities are added to $ErRh_4B_4$. In the measurement on $Y_xEr_{1-x}Rh_4B_4$ (Ref. 11) it is observed that for low concentrations of Y (i.e., $x \ll y$), the impurity concentration dependence of the magnetic transition temperature is given by

$$T_m^x=T_m(1-x) . \tag{4.2}$$

This can be used with Eqs. (2.17), (2.27), and (2.33) to obtain the x dependence of the superconducting transition temperature T_c^x,

$$\frac{I^2}{g_0}=\frac{4\pi g_0N(0)}{c^{(a)}}\frac{(1-t_m^{(a)})\{1+t_m^{(a)}[d_f^{(a)}(1+\alpha)-1]\}}{Zt_m^{(a)}}\frac{(d/dx)\ln T_c(x)}{1+(d/dx)\ln T_c(x)}\bigg|_{x=0} , \tag{4.3}$$

where Z is given by

$$Z=2+\frac{1-t_m^{(a)}}{1-t_m^{(c)}}\left[\frac{t_m^{(a)}}{t_m^{(b)}}\right]\frac{d_f^{(a)}(1+\alpha)+\epsilon^{(a)}(t=1)}{d_f^{(c)}(1+\alpha)+\epsilon^{(c)}(t=1)} , \tag{4.4}$$

and the various dimensionless parameters are those defined in Eqs. (2.35c) and (2.35f).

The value of $(d/dx)\ln T_c(x)$ may be estimated from experiment[11] as

$$\frac{d}{dx}\ln T_c(x)\bigg|_{x=0}\simeq 0.14 . \tag{4.5}$$

Thus Eq. (4.3) together with Eq. (4.4) may be used to estimate the value of I^2/g_0 once $d_f^{(a)}$ and α are specified.

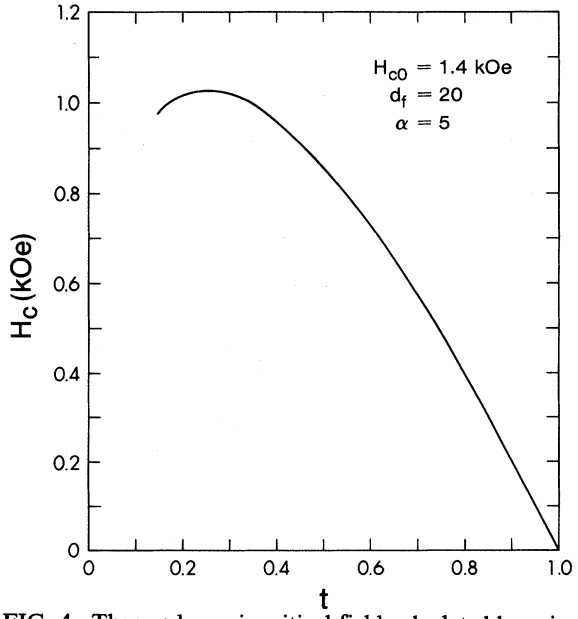

FIG. 4. Thermodynamic critical field calculated by using the parameters given in Tables II and III(a) *including* the effect of the spin fluctuations.

The remaining parameter $d^{(a)}$ may be estimated from the coexistence temperature T_p, since T_p is given by[12]

$$T_p\simeq T_m-2\left[\frac{4\pi c^{(a)}}{D\lambda_L^{-2}}\right]^{1/2}$$
$$=T_m\left[1-2\left[\frac{c^{(a)}}{d^{(a)}}\right]^{1/2}\right] . \tag{4.6}$$

The value of T_p shown in Table I is estimated from the neutron scattering data on single-crystal $ErRh_4B_4$.[13] The parameters α and d_f cannot as yet be obtained from any experimental values and are therefore adjusted to provide a reasonable overall fit to the data. If we choose $\alpha=5$ and $d_f\simeq 20$, then the thermodynamic critical field may be calculated as a function of temperature. The results are shown in Fig. 4. The resultant value of $\bar{I}(\equiv Ig_J J\mu_B N/\Delta_0)$ is 3.555. This gives

$$\mathcal{J}=\left[\equiv I\frac{g_J-1}{g_J\mu_B N}\right]\simeq 1.5\times 10^{-3}\ \mathrm{eV}$$

somewhat lower than other estimates.[14] The experimental parameters are summarized in Table I.

V. UPPER AND LOWER CRITICAL FIELDS FOR $ErRh_4B_4$

In this section we wish to present the results of our numerical calculations of the upper and lower critical fields based on the parameters discussed in the preceding section and compare them with the recently published single-crystal data for $ErRh_4B_4$.[1] We present the results of two separate analyses. In the first analysis we simply apply the parameters determined in Sec. IV and presented in Table II together with those in Table III(a), and proceed as outlined in Secs. II and III to compute the critical fields. In the second analysis we neglect the effect of the scaling and modify the parameters κ_B and $\bar{I}$ to obtain a good fit to the experimentally observed upper and lower

TABLE II. Nondimensional parameters used in theoretical calculations.

$t_m^{(a)}=T_m^{(a)}/T_c=0.115$	$g_0N(0)=0.3$
$t_m^{(c)}=T_m^{(c)}/T_c=-2.300$	$d=(D/T_m\lambda_{L0}^2)=0.452\times10^{-2}$
$t_p=T_p/T_c=0.092$	
$c^{(a)}=4\pi C/T_m^{(a)}=2.312$	$J=7.5$

The parameters d_f, U, and $\bar{I}$ are defined as

$$d_f=4Dk_f^2/T_m^{(a)}$$
$$u=g_J\mu_BJN/(\phi/\lambda_{L0}^2)$$
$$\bar{I}=\frac{Ig_J\mu_BJN}{\Delta_0}=\left[\frac{8\pi^5}{3}g_0N(0)\frac{I^2}{g_0}\right]^{1/2}\frac{u}{\kappa_B}$$

critical fields. The parameters used are presented in Table II, together with those in Table III(b).

The reason for the two separate analyses is twofold. First, there is good reason to suppose that introducing the spin fluctuations by means of the effective coupling constant described in Sec. II probably overestimates their effects, particularly at lower temperature. Therefore, it is interesting to compare this analysis with one in which the effect of the fluctuations is underestimated. Such a situation is obviously realized if they are neglected completely. The second reason is that a comparison of the two numerical analyses helps to illustrate the role played by the spin fluctuations.

The numerical results for the upper and lower critical fields H_{c2}, H_{c2}^0, and $H_{c1}(\simeq H_{c1}^0)$, including the effects of the spin fluctuations, are shown in Fig. 5 for the easy-axis direction, together with the single-crystal measurements on $ErRh_4B_4$.[1] The upper solid line shows H_{c2} $(=H_{c2}^0$ when the transition to the normal state is second order). The dashed line shows the computed H_{c2}^0 curve when the transition from the mixed state to the normal state is first order. It should be noted that the agreement with experiment is rather good. Not only are the calculated values in good agreement with the experimental values but also, the temperature at which the transition at H_{c2} changes from second to first order is in good agreement with the experimental value of $t\simeq0.4$. With the use of the same parameter, the hard-axis upper critical-field H_{c2} curve is shown in Fig. 6 with the single-crystal measurements. The lower critical-field curve is similar to that obtained for the easy axis. The decrease in H_{c2} for low temperatures arises from the decrease in the condensation energy arising from the localized-spin fluctuations. The agreement with experiment is reasonably good.

The results of the numerical analyses of the upper and lower critical fields H_{c2}, H_{c2}^0, and $H_{c1}(\simeq H_{c1}^0)$, neglecting the effect of the spin fluctuations, are shown in Fig. 7 for the easy-axis direction, together with the corresponding single-crystal measurements.[1] Again, the upper solid line denotes H_{c2} and dashed line denotes H_{c2}^0. The upper critical field in the case of the hard axis is shown in Fig. 8 with the corresponding single-crystal measurements. Again, the agreement is quite acceptable.

A number of important conclusions may be drawn from these results. First, it would appear that both the measured upper and lower critical-field curves along both the hard and easy axes may quantitatively be described by using existing analytical methods suitably modified to include the d-f interaction and by using a set of parameters consistent with many other measurements. Second, it has become apparent in the course of our computations that it is difficult, solely on the basis of the easy-axis upper and lower critical-field curves, to distinguish between the ef-

TABLE III. (a) Parameters used in calculation *including* the effect of the spin fluctuations. (b) Parameters used in calculation *neglecting* the effect of the spin fluctuations.

(a)	(b)
$\kappa_B=4$	$\kappa_B=3.5$
$d_f=20$	$\bar{I}=4.285$
$\alpha=5$	
This gives	
$I^2/g_0\simeq10.15$, $\bar{I}=3.555$	

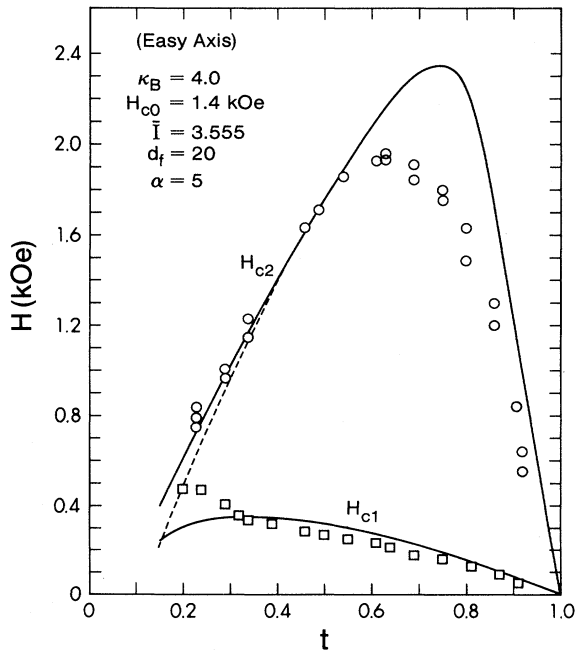

FIG. 5. Easy-axis upper and lower critical fields H_{c2} and H_{c1} calculated by using the parameters given in Tables II and III(a) *including* the effect of the spin fluctuations. The dashed line represents H_{c2}^0. Also shown are the experimental measurements after Crabtree *et al.* (Ref. 1).

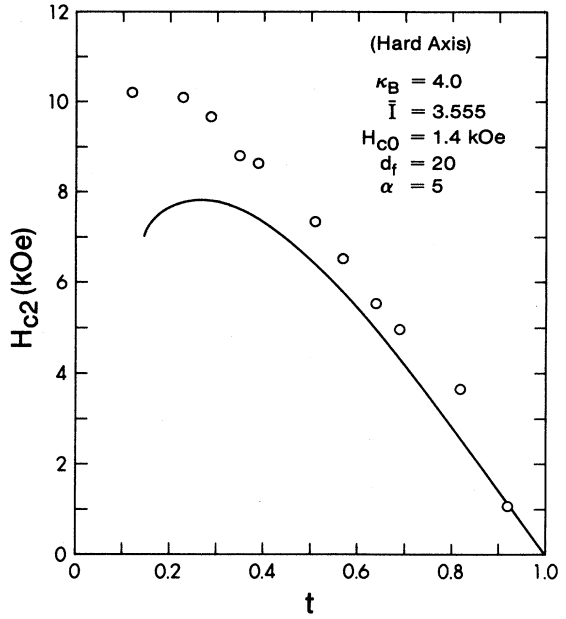

FIG. 6. Hard-axis upper critical field H_{c2} calculated by using the parameters given in Tables II and III(a) *including* the effect of the spin fluctuations. Also shown are the experimental measurements after Crabtree *et al.* (Ref. 1).

fects of the electron polarization and the scattering by the spin fluctuations. Indeed, qualitatively similar curves can be obtained with slightly modified parameters with or without the effect of the fluctuations or the polarization. If, however, one considers the hard-axis critical-field curves with the same sets of parameters, marked differences appear depending on which effects are included. This is seen to some extent by comparing the curves shown in Figs. 5 and 6 with those given in Figs. 7 and 8. This indicates the crucial role of the single-crystal measurements in the understanding and interpretation of magnetic properties of these materials.

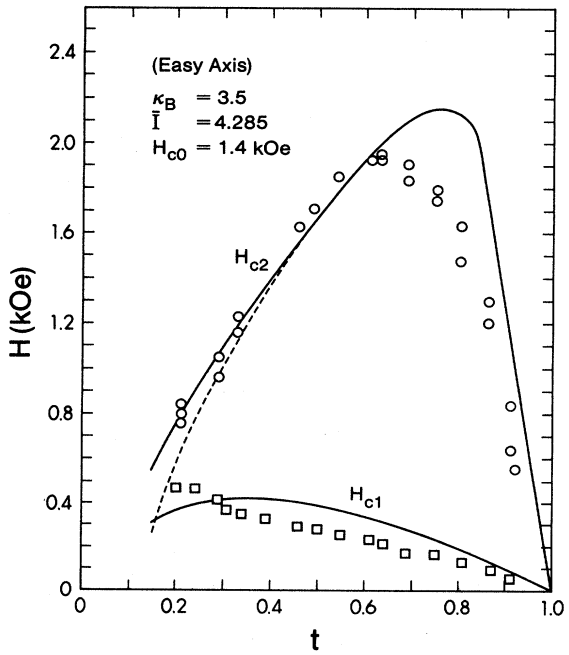

FIG. 7. Easy-axis upper and lower critical fields H_{c2} and H_{c1} calculated by using the parameters given in Tables II and III(b) *neglecting* the effect of the spin fluctuations (i.e., $s=1$). The dashed line represents H_{c2}^0. Also shown are the experimental measurements after Crabtree *et al.* (Ref. 1).

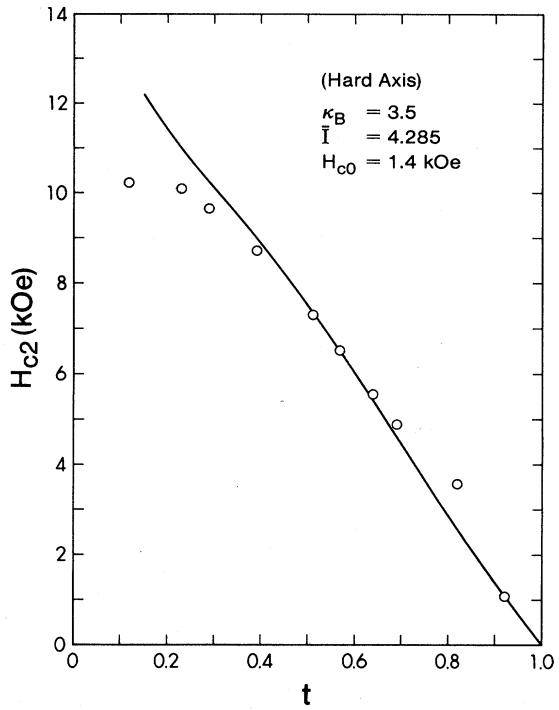

FIG. 8. Hard-axis upper critical field H_{c2} calculated by using the parameters given in Tables II and III(b) *neglecting* the effect of the spin fluctuation (i.e., $s=1$). Also shown are the experimental results after Crabtree *et al.* (Ref. 1).

VI. MAGNETIZATION CURVES

In addition to the upper and lower critical-field curves discussed in the preceding section, detailed magnetization measurements have been performed with single-crystal $ErRh_4B_4$. The resulting magnetization curves show the appearance of a first-order phase transition between the mixed state and the normal state at low temperatures ($T \lesssim 0.4$). From the analysis summarized in Sec. III, the bulk magnetization is given by[15]

$$4\pi M = n\phi - H(n) , \tag{6.1}$$

where $H(n)$ is computed from Eq. (3.12b) with the expression for the free energy given in Eq. (3.9).

The results of several magnetization curves computed for various values of the reduced temperature t are presented with the use of the parameters given in Table II, together with those of Table III(a), *including* the effect of the spin fluctuations in Fig. 9. Two features are worth noting with regard to these curves. First, the magnetization for $t=0.4$ clearly demonstrates a convex nature around H_{c2}, similar to that observed in the experimental magnetization curves.[2] Furthermore, as the temperature is lowered the convex nature of the magnetization be-

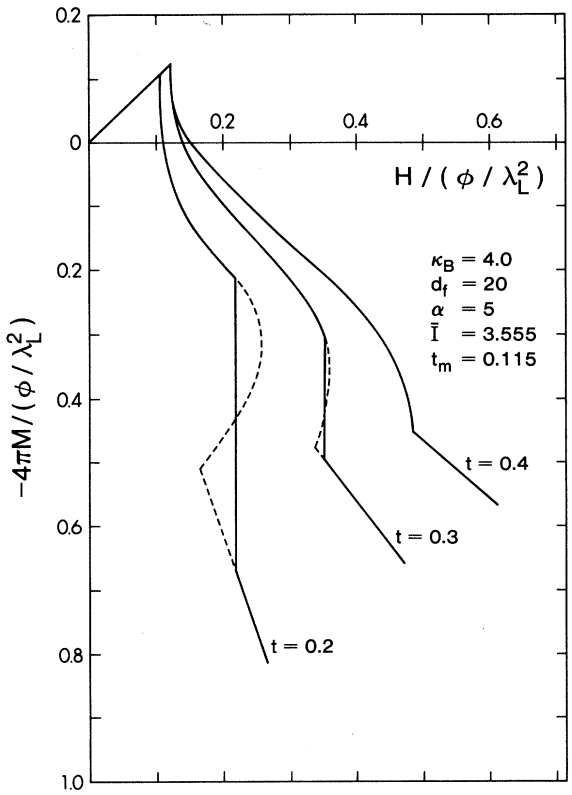

FIG. 9. Easy-axis-magnetization curves for various values of the reduced temperature calculated by using the parameters given in Tables II and III(a) *including* the effect of the spin fluctuations.

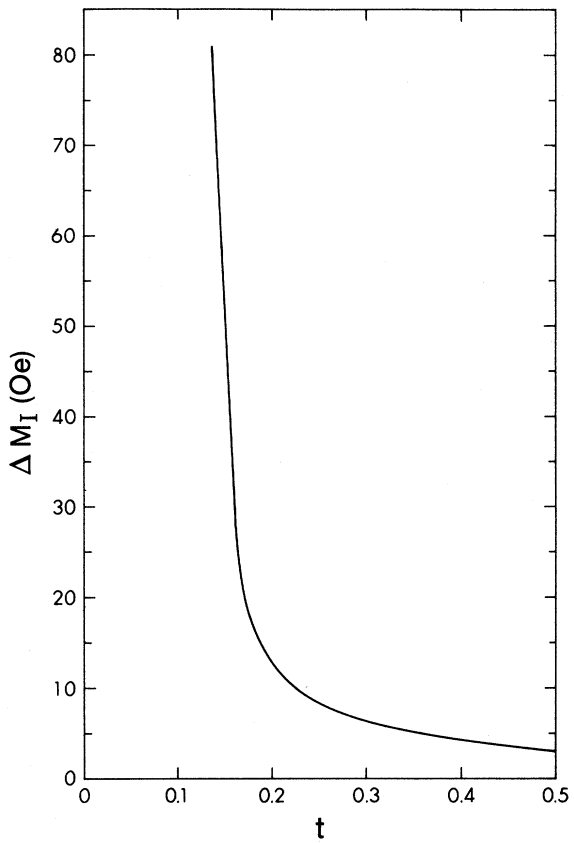

FIG. 10. Jump in the magnetization at H_{c1} and $\Delta M_{\rm I}$, calculated from curves similar to those shown in Fig. 9.

comes so pronounced that the curve exhibits a supercooling portion around H_{c2}^0 and hence a first-order transition at H_{c2}. This is clearly seen in the curves calculated for $t=0.3$ and 0.2. Second, the magnetization curves also show the appearance at low temperature of a first-order transition at H_{c1} as the temperature is lowered. This becomes quite pronounced below $t\simeq 0.15$. The appearance of the first-order transition at H_{c1} may be attributed to two reasons: the modification of the vortex-vortex interaction induced by the dipole interaction[16] and the temperature- and field-dependent change in the superconducting current and the condensation energy arising from the scattering by the localized-spin fluctuations.

These results indicate that the sequence of phase transitions as the temperature is lowered is given by

$$\text{type II}_{2,2}\rightarrow\text{type II}_{1,2}\rightarrow\text{type II}_{1,1}\rightarrow\text{type I}\ ,$$

where we have defined the type $\text{II}_{i,j}$ $(i,j=1,2)$ in the following way: $i=1$ $(j=1)$ means a first-order transition at H_{c1} (H_{c2}) and $i=2$ $(j=2)$ implies a second-order transition at H_{c1} (H_{c2}).

Regarding the jump in the magnetization at H_{c1}, which will be referred to as ΔM_I, and illustrated in Fig. 10, it should be noted that for $t\gtrsim 0.15$ the calculated jump is relatively small. Given the difficulties inherent in the measurement of the magnetization curve around H_{c1} that arise from the flux pinning and the fact that the slope of the magnetization curve around H_{c1} would be infinite were it not for the pinning, it is quite likely that such a small jump would be extremely difficult to observe.

The results of several magnetization curves computed for various values of the reduced temperature by using the parameters given in Table II together with those in Table III(b) and neglecting the effect of the spin fluctuations, are presented in Fig. 11. The behavior in the vicinity of H_{c2} is seen to be qualitatively similar to that obtained in the previous analysis. However, the transition at H_{c1} was found to be second order, indicating that the sequence of the transitions as the temperature is lowered in this instance is given by

$$\text{type II}_{2,2}\rightarrow\text{type II}_{2,1}\rightarrow\text{type I}\ .$$

The jump in the magnetization at H_{c2}, which will be denoted by $\Delta M_{\rm II}$, may be obtained from the magnetization curves. The resultant curves, together with some experimental points, are shown in Fig. 12. The lower curve (labeled A) is that obtained by using the parameters of Table I including the spin fluctuations; the upper curve is that obtained by using the parameters of Table II neglecting the spin fluctuations. The points are somewhat lower than those observed experimentally.[2]

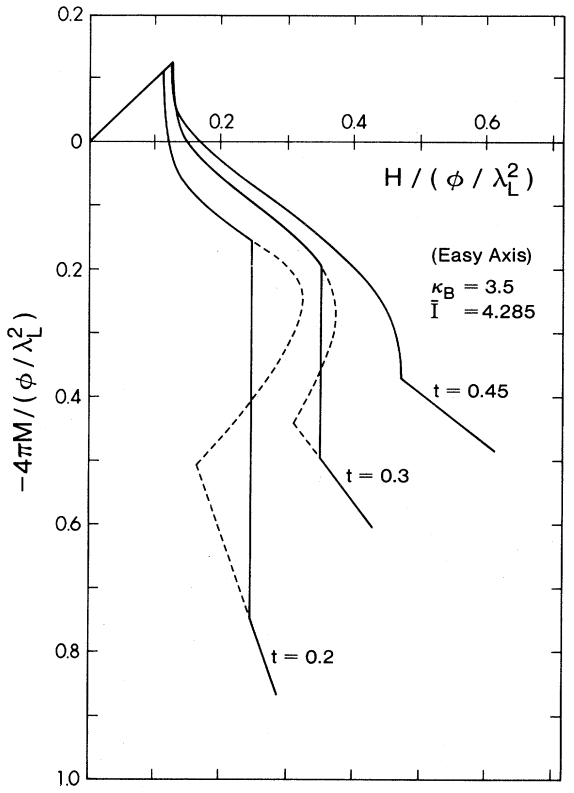

FIG. 11. Easy-axis-magnetization curves for various values of the reduced temperature calculated by using the parameters given in Tables II and III(b) *neglecting* the effect of the spin fluctuations.

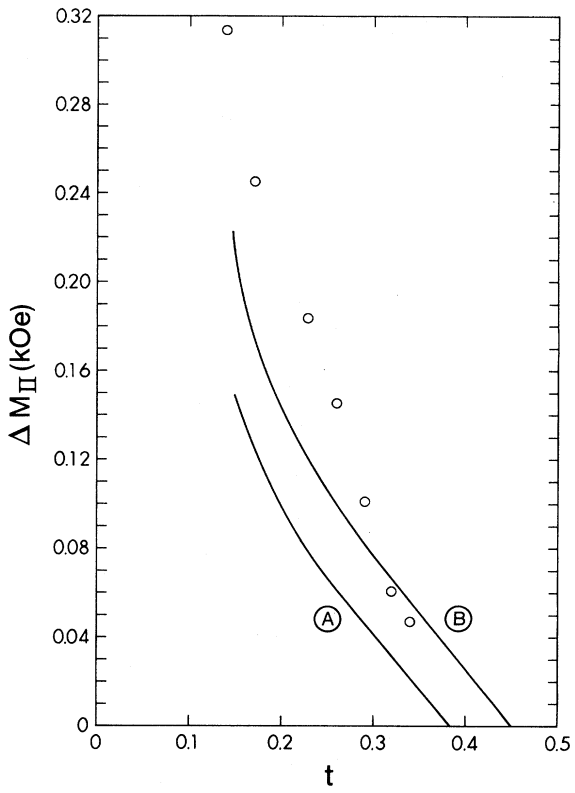

FIG. 12. Jump in the magnetization at H_{c2} and ΔM_{II}. The lower curve (labeled A) is calculated from the parameters given in Tables II and III(a) *including* the effect of the spin fluctuations. The upper curve (labeled B) is calculated from the parameters given in Tables II and III(b) *neglecting* the effect of the spin fluctuations.

Several features are worth noting. First, the appearance of the first-order transition at H_{c2} appears to be a direct consequence of the polarization of the superconducting electrons induced by the *d-f* interaction. This result is consistent with other calculations[17] which show that the magnetization curve develops a convex curvature around H_{c2}, although no calculations, apart from those presented here, have considered the temperature domain where the transition becomes type $II_{i,1}$. The second point worth noting is the fact that while the scaling effect induced by the localized-spin fluctuations does not play a crucial role in determining the nature of the transition around H_{c2}, it does, together with the dipole interaction, have important consequences regarding the nature of the transition around H_{c1}. This is clearly shown by the fact that the jump in the magnetization appearing in Fig. 7 disappears when the scaling effect is neglected. Therefore, in order to draw any precise conclusion regarding the nature of the transition at H_{c1}, it is necessary to examine, in more detail, the pair-breaking effect of the localized-spin fluctuations and the long-range structure of the vortex current.

VII. CONCLUSIONS

The results of this analysis reveal that many of the recently observed magnetic properties of $ErRh_4B_4$ may be adequately described in terms of the existing analysis provided the *d-f* interaction is included. This includes the region where the transition to the normal state at H_{c2} is first order and the observed magnetization curve is discontinuous. It is also important to note that reasonably good agreement with both the hard- and easy-axis critical-field curves was obtained with a single value of κ_B. This indicates that the large anisotropy observed in critical-field curves is largely due to the anisotropy in the magnetic interaction between the Er ions rather than any anisotropy in the properties of the superconducting electrons. This seems to be supported by experimental measurements.[10]

The results of our analysis also show that while the scaling induced through the scattering of the electrons by the spin fluctuations can substantially affect the condensation energy and the detailed nature of transition around H_{c1}, its effect on the qualitative behavior of the upper critical-field curves and of the magnetization curve in the neighborhood of H_{c2} is negligible. Indeed, as is shown when the scaling effect is neglected, one may obtain good quantitative agreement regarding the latter two quantities by a rather minor modification of the parameters used. This is somewhat unfortunate since the measurement of the magnetization curve around H_{c1} and the temperature dependence of the condensation energy in $ErRh_4B_4$ is ex-

tremely difficult due to the amount of flux pinning present, making it very difficult to draw any definite conclusions regarding the effect of the spin fluctuations on the superconducting properties from the magnetization measurements. A corollary of this last observation is that the dominant effect arising from the *d-f* interaction observed in the existing magnetization measurements on $ErRh_4B_4$ arises from the polarization of the superconducting electrons by the Er moments.

ACKNOWLEDGMENTS

The authors would like to thank Dr. M. Tachiki, Dr. G. W. Crabtree, and Dr. T. Koyama for valuable discussions. This work was supported by the Natural Sciences and Engineering Research Council of Canada, and the Dean of Faculty of Science, University of Alberta (Edmonton, Alberta, Canada). One of the authors (J.P.W.) was supported by the Alberta Heritage Scholarship Fund.

[1]G. W. Crabtree, F. Berhoozi, S. A. Cambell, and D. G. Hinks, Phys. Rev. Lett. **49**, 1342 (1982).

[2]F. Berhoozi, G. W. Crabtree, S. A. Cambell, and D. G Hinks, Phys. Rev. B **27**, 6849 (1983).

[3]H. Matsumoto, R. Teshima, H. Umezawa, and M. Tachiki, Phys. Rev. B **27**, 158 (1983).

[4]H. Matsumoto, H. Umezawa, and J. P. Whitehead, Phys. Rev. B **30**, 1294 (1984).

[5]I. Shapira, M. N. Shah, and H. Umezawa, Physica (Utrecht) **84B**, 213 (1976).

[6]M. Tachiki, A. Kotani, H. Matsumoto, and H. Umezawa, Solid State Commun. **31**, 927 (1979).

[7]H. Umezawa, H. Matsumoto, and M. Tachiki, *Thermo Field Dynamics and Condensed States* (North-Holland, Amsterdam, 1982).

[8]G. W. Crabtree (private communication).

[9]L. D. Woolf, D. C. Johnston, H. B. MacKay, R. W. McCallum, and M. B. Maple, J. Low Temp. Phys. **35**, 651 (1979).

[10]F. Berhoozi (private communication).

[11]K. Okuda, Y. Nakakura, and K. Kadowaki, Solid State Commun. **32**, 185 (1979).

[12]H. Matsumoto, H. Umezawa, and M. Tachiki, Solid State Commun. **31**, 157 (1979).

[13]S. K. Sinha, G. W. Crabtree, D. G. Hinks, and H. Mook, Phys. Rev. Lett. **48**, 950 (1982).

[14]See, for example, M. B. Maple, *Ternary Superconductors,* edited by G. K. Shenoy, B. D. Dunlap, and F. Y. Fradin (Elsevier, New York, 1981), p. 131.

[15]Here we use M to denote the total bulk magnetization per unit volume as distinct from $\langle M_3 \rangle$ which denotes the net magnetic moment per unit volume arising solely from the polarization of the magnetic ions.

[16]M. Tachiki, H. Matsumoto, and H. Umezawa, Phys. Rev. B **20**, 1915 (1979).

[17]O. Sakai, M. Suzuki, S. Maekawa, M. Tachiki, G. W. Crabtree, and F. Berhoozi, J. Phys. Soc. Jpn. **52**, 134 (1983); T. Koyama, S. Maekawa, and M. Tachiki, *ibid.* **52**, 1750 (1983).